JOURNAL OF VIROLOGY, Feb. 2001, p. 1459–1475 Vol. 75, No. 3
0022-538X/01/$04.00+0 DOI: 10.1128/JVI.75.3.1459–1475.2001
Copyright © 2001, American Society for Microbiology. All Rights Reserved.

Reovirus σNS Protein Is Required for Nucleation of Viral Assembly Complexes and Formation of Viral Inclusions

MICHELLE M. BECKER,[1,2] MEHMET I. GORAL,[1,2,3] PAUL R. HAZELTON,[4] GEOFFREY S. BAER,[1,2] STEVEN E. RODGERS,[1,2] EARL G. BROWN,[5] KEVIN M. COOMBS,[4] AND TERENCE S. DERMODY[1,2,3]*

Departments of Microbiology and Immunology[1] and Pediatrics[3] and Elizabeth B. Lamb Center for Pediatric Research,[2] Vanderbilt University School of Medicine, Nashville, Tennessee 37232, and Department of Medical Microbiology and Infectious Diseases, University of Manitoba, Winnipeg, Manitoba,[4] and Department of Biochemistry, Microbiology and Immunology, Faculty of Medicine, University of Ottawa, Ottawa, Ontario,[5] Canada

Received 12 June 2000/Accepted 26 October 2000

Progeny virions of mammalian reoviruses are assembled in the cytoplasm of infected cells at discrete sites termed viral inclusions. Studies of temperature-sensitive (*ts*) mutant viruses indicate that nonstructural protein σNS and core protein μ2 are required for synthesis of double-stranded (ds) RNA, a process that occurs at sites of viral assembly. We used confocal immunofluorescence microscopy and *ts* mutant reoviruses to define the roles of σNS and μ2 in viral inclusion formation. In cells infected with wild-type (wt) reovirus, σNS and μ2 colocalize to large, perinuclear structures that correspond to viral inclusions. In cells infected at a nonpermissive temperature with σNS-mutant virus *tsE320*, σNS is distributed diffusely in the cytoplasm and μ2 is contained in small, punctate foci that do not resemble viral inclusions. In cells infected at a nonpermissive temperature with μ2-mutant virus *tsH11.2*, μ2 is distributed diffusely in the cytoplasm and the nucleus. However, σNS localizes to discrete structures in the cytoplasm that contain other viral proteins and are morphologically indistinguishable from viral inclusions seen in cells infected with wt reovirus. Examination of cells infected with wt reovirus over a time course demonstrates that σNS precedes μ2 in localization to viral inclusions. These findings suggest that viral RNA-protein complexes containing σNS nucleate sites of viral replication to which other viral proteins, including μ2, are recruited to commence dsRNA synthesis.

Mammalian reoviruses are nonenveloped, icosahedral viruses that contain a genome of 10 double-stranded (ds) RNA gene segments. Reovirus virions consist of two concentric protein shells, outer capsid and core, which are assembled from eight unique structural proteins. After penetration of the virus into the cytoplasm and transcription and translation of viral RNA (reviewed in reference 25), assembly of progeny reovirus virions is thought to proceed along a pathway involving a series of assembly intermediates. Particles that contain reovirus mRNAs in association with viral proteins μNS, σNS, and σ3 have been suggested to represent the first complexes in reovirus assembly (3). Particles that are engaged in minus-strand synthesis have been isolated from infected cells and probably represent the next step in the assembly pathway (21). Assortment of the 10 gene segments appears to occur concomitantly with synthesis of dsRNA within nascent viral particles (3); however, the mechanism ensuring that the 10 unique dsRNA segments are packaged into each newly formed particle is not known (reviewed in reference 18). Nascent dsRNA-containing particles are competent for transcription of viral mRNA (22, 37, 48), and transcription within these particles accounts for the majority of the mRNA in reovirus-infected cells (38, 43, 44). Reovirus assembly is completed by the addition of outer-capsid proteins, resulting in formation of mature, double-shelled virions (22).

A precise understanding of the steps in reovirus assembly has not been achieved, and the exact location within the cellular environment in which these processes take place is unknown. It is generally thought that reovirus particle morphogenesis leading to formation of viral progeny occurs within viral inclusions. However, it is possible that progeny virions are assembled in the cytoplasm of infected cells and then are collected to form inclusion structures. Viral inclusions have been studied by a variety of microscopic techniques and first appear by phase-contrast microscopy as dense granules scattered throughout the cytoplasm. As infection progresses, these granules coalesce and localize about the nucleus, eventually forming perinuclear inclusions (11). Viral inclusions contain several types of filaments (35), dsRNA (36), viral proteins (11), and complete and incomplete viral particles (11). In contrast to cytoplasmic sites of replication used by several other viruses, reovirus inclusions are not associated with membranes or other cellular organelles (14, 31).

Temperature-sensitive (*ts*) reovirus mutants have been used to investigate the functions of individual viral proteins (reviewed in reference 6). In several cases, the *ts* phenotypes of these mutants have been mapped to discrete gene segments by analysis of reassortant viruses (23, 28–30) or definition of complementation groups (1, 2, 9). Several of these mutants exhibit blocks to viral replication prior to synthesis of dsRNA. One such mutant, *tsE320* (9), contains a genetic defect that was previously mapped by reassortant analysis to the S3 gene segment (30), which encodes nonstructural protein σNS (20, 23). The σNS protein has strong affinity for single-stranded RNA (12, 13, 17, 32, 39), including reovirus mRNAs (13, 17, 32, 39). During infection at a nonpermissive temperature, *tsE320* synthesizes less than 1% of the level of dsRNA relative to infec-

* Corresponding author. Mailing address: Lamb Center for Pediatric Research, D7235 MCN, Vanderbilt University School of Medicine, Nashville, TN 37232. Phone: (615) 343-9943. Fax: (615) 343-9723. E-mail: terry.dermody@mcmail.vanderbilt.edu.

TABLE 1. Properties of σNS-specific MAbs

Antibody	Isotype	Result obtained by[a]:			
		ELISA	Immunoblotting	Immunofluorescence	Immunoprecipitation
1D8	IgM, κ	+	ND	ND	ND
2A9	IgG1, κ	+	−	+	+
2F5	IgG1, κ	+	−	+	+
2H7	IgG2a, κ	+	+	+	−
3E10	IgG1, κ	+	+	+	+

[a] ND, not determined; +, positive; −, negative.

tion at a permissive temperature (8, 10). The nucleotide sequence of the *tsE320* S3 gene differs from the wild-type (wt) type 3 Dearing (T3D) S3 sequence at a single nucleotide position, which results in a methionine-to-threonine substitution at position 260 in the deduced amino acid sequence of σNS (45). The block to dsRNA synthesis exhibited by *tsE320* has not been defined.

Another dsRNA-negative *ts* mutant, *tsH11.2* (7), contains a genetic defect that was mapped by reassortant analysis to the M1 gene segment (4), which encodes virion structural protein μ2 (20, 24). The μ2 protein is present in the viral core in approximately 20 copies per virion (5). The μ2-encoding M1 gene determines strain-specific differences in both the temperature optimum and the kinetics of reovirus transcription in vitro (46) and is one of two reovirus genes that modulates in vitro nucleoside triphosphatase activity (26). In addition, the M1 gene segregates with strain-specific differences in kinetics of viral inclusion formation (19). During infection at a nonpermissive temperature, *tsH11.2* produces approximately 0.1% of the level of dsRNA relative to infection at a permissive temperature (4). The nucleotide sequence of the *tsH11.2* M1 gene has two changes compared to wt T3D, each resulting in a change in the deduced amino acid sequence of μ2: a methionine-to-threonine change at amino acid 399 and a proline-to-histidine change at amino acid 414 (4). As with *tsE320*, the block to viral genome replication exhibited by *tsH11.2* has not been defined.

Experiments described in this report were designed to provide new information about the roles of σNS and μ2 in formation of viral inclusions. To facilitate these studies, we generated a new panel of σNS-specific monoclonal antibodies (MAbs) and isolated new reassortant viruses from crosses of wt reovirus strain type 1 Lang (T1L) and σNS-mutant strain *tsE320*. Subcellular localization of reovirus proteins was examined at different times postinfection in cells infected with wt reovirus, *tsE320*, and *tsH11.2* at permissive and nonpermissive temperatures. The findings demonstrate that viral RNA-protein complexes containing σNS nucleate sites of viral replication to which μ2 and other viral proteins are recruited to initiate dsRNA synthesis.

MATERIALS AND METHODS

Cells and viruses. Mouse L929 (L) cells were grown in either suspension or monolayer cultures in Joklik's modified Eagle's minimal essential medium (Irvine Scientific, Santa Ana, Calif.) that was supplemented to contain 5% fetal calf serum (Intergen, Purchase, N.Y.), 2 mM L-glutamine, 100 U of penicillin G per ml, 100 μg of streptomycin per ml, and 250 ng of amphotericin B per ml (Irvine Scientific). Sp2/0-Ag14 myeloma cells (American Type Culture Collection, Manassas, Va.) and hybridoma cells were grown in Dulbecco's modified Eagle medium (DMEM; Gibco, Grand Island, N.Y.) supplemented to contain either 10% (DMEM-10) or 20% (DMEM-20) fetal calf serum, 20 mM HEPES (Gibco), 1 mM sodium pyruvate (Gibco), 0.1 mM nonessential amino acids (Gibco), 2 mM L-glutamine, and 100 U of penicillin, 100 μg of streptomycin, and 250 ng of amphotericin per ml. Hybridoma cells were selected in DMEM-20 containing 0.1 mM hypoxanthine, 0.4 μM aminopterin, and 1 μM thymidine (HAT medium) and subcloned in DMEM-20 supplemented to contain 5% hybridoma cloning factor (Igen, Gaithersburg, Md.).

Reovirus wt strains T1L and T3D and mutant *tsH11.2* are laboratory stocks. Mutant *tsE320* was grown from stocks originally obtained from B. N. Fields (9). Second- or third-passage L-cell lysate stocks of twice-plaque-purified isolates of each strain were used for subsequent studies. Virus titers were determined by plaque assay on L-cell monolayers as previously described (16).

Isolation of reassortant viruses and identification of genes responsible for *ts* phenotypes. Reassortant viruses were isolated from mixed infections of T1L and *tsE320* by a previously described technique with minor modifications (16). Cells were incubated at 32°C for all steps in the isolation procedures. Subconfluent L-cell monolayers were coinfected with each parental strain at a multiplicity of infection (MOI) of 5 PFU per cell and incubated for 33 h. Cell lysates were prepared by performing three cycles of freezing and thawing, and titers of virus in cell lysates were determined by plaque assay. Isolated plaques were picked, and putative reassortant viruses were amplified by two passages in L cells. Genotypes of putative reassortants were determined as previously described (16).

Cloning and sequencing of viral cDNA. Reovirus genomic dsRNA was purified from second-passage L-cell lysate stocks by previously described techniques (15). Oligodeoxynucleotide primers 5′-AAGTCACGCCTGTCGTCGTC-3′ and 5′-ACCACCAAGACACCGGCACA-3′, which correspond to the 5′ and 3′ termini of the S3 gene, respectively, were used to generate cDNA clones from genomic dsRNA. Genomic dsRNA was incubated in 90% dimethyl sulfoxide at 50°C for 45 min, ice-cold primers were annealed to the melted template, and cDNAs were generated using avian myeloblastosis virus reverse transcriptase (Roche Molecular Biochemicals, Indianapolis, Ind.). PCR was performed with *Taq* DNA polymerase (Perkin-Elmer, Branchburg, N.J.) for 34 cycles, using a program of denaturation at 95°C for 2 min, annealing at 50°C for 2 min, and synthesis at 72°C for 3 min. PCR was completed by a synthesis step at 72°C for 20 min. Resultant cDNAs were cloned into the pCRII vector (Invitrogen, San Diego, Calif.). Unambiguous sequences of 1,136 nucleotides of the S3 gene, including the entire open reading frame (ORF) of σNS, were determined by dideoxy chain termination using T7 DNA polymerase (United States Biochemical, Cleveland, Ohio). Independent *tsE320* S3 cDNA clones generated from two reverse transcription (RT)-PCR assays were used as templates in the sequencing experiments.

Expression and purification of recombinant σNS protein. A cDNA of the T3D reovirus σNS ORF was generated by RT-PCR of purified reovirus dsRNA. Primers corresponding to terminal sequences of the σNS ORF appended with restriction enzyme cleavage sites were used for RT-PCR. Restriction sites engineered into the S3 cDNA were used for directional cloning of the σNS ORF into the pQE-30 expression vector (Qiagen, Valencia, Calif.) in frame and 5′ to a sequence encoding six histidine residues. The recombinant pQE-30 vector was used to transform *Escherichia coli* M15(pREP4) (Qiagen). Expression of σNS-His was induced with 0.3 mM isopropyl-β-D-thiogalactopyranoside (IPTG). After 4 h of growth following induction, cells were centrifuged to form a pellet, resuspended in lysis buffer containing 1% Triton X-100 (Roche), and lysed by sonication. σNS-His was purified by metal chelate affinity chromatography, using a nitrilotriacetate resin charged with Ni^{2+} ions, and eluted with imidazole (Qiagen).

The cDNA of the T3D σNS ORF also was subcloned into the pMAL-c2 vector to express σNS as a carboxy-terminal fusion protein with maltose-binding protein (MBP) (New England Biolabs, Beverly, Mass.). The recombinant pMAL-c2 vector was used to transform *E. coli* DH5α, and these cells were induced to express the fusion protein by the addition of 0.3 mM IPTG. After 4 h of growth

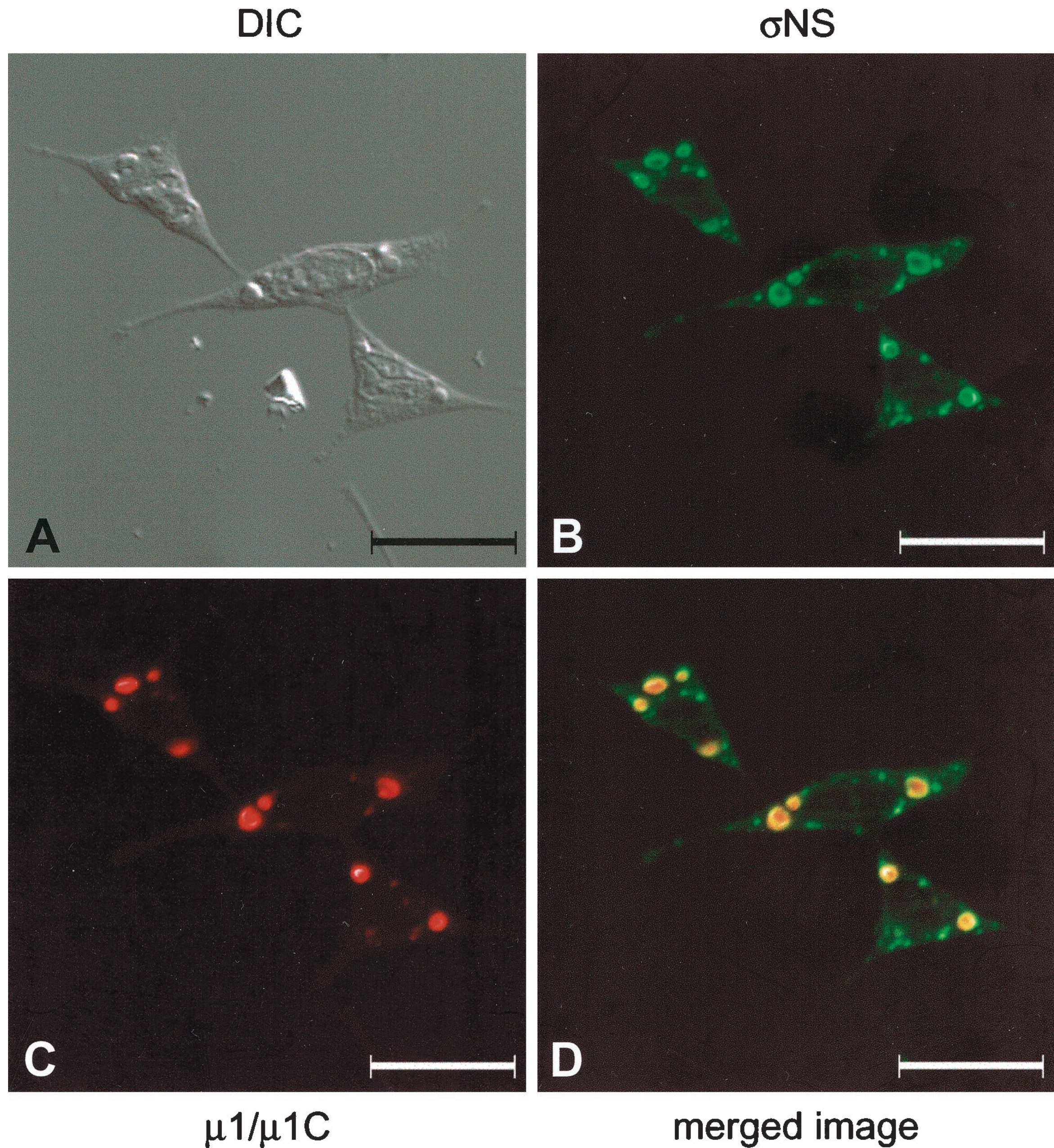

FIG. 1. Subcellular localization of reovirus σNS and μ1/μ1C proteins in cells infected with reovirus strain T3D. L cells were infected with T3D at an MOI of 10 PFU per cell and incubated at 37°C for 18 h. Cells were stained for σNS by using a σNS-specific polyclonal antiserum (B) and for μ1/μ1C by using μ1/μ1C-specific MAb 8H6 (C) as primary antibodies followed by Alexa Fluor 488 goat anti-rabbit IgG and Alexa Fluor 546 goat anti-mouse IgG, respectively, as secondary antibodies. Images were obtained by using a confocal microscope. The σNS protein is colored green, and the μ1/μ1C protein is colored red. (A) A DIC image of the field was obtained. (D) In the merged image, colocalization of σNS and μ1/μ1C is indicated by the yellow color. Images were processed using Adobe Photoshop. Bars, 25 μm.

following induction, cells were centrifuged to form a pellet, resuspended, and frozen at −20°C in column buffer (20 mM Tris-HCl [pH 7.4], 200 mM NaCl, 1 mM EDTA). Cells were lysed by sonication, lysates were clarified by centrifugation, and MBP-σNS was purified by affinity chromatography using an amylose resin (New England Biolabs).

Generation of rabbit antiserum. Rabbit σNS-specific antiserum was produced by inoculating a New Zealand White rabbit with approximately 100 μg of σNS-His in incomplete Freund's adjuvant, followed by 100-μg booster doses at 2, 3, and 7 weeks postinoculation (Cocalico, Reamstown, Pa.). Antiserum was obtained from the rabbit 4 weeks after the last boost and incubated at 56°C for 1 h prior to use. Rabbit μ2-specific antiserum was produced as previously described (49).

Generation and characterization of σNS-specific MAbs. BALB/c mice were inoculated intraperitoneally with 50 μg of σNS-His combined with Ribi adjuvant (Ribi, Hamilton, Mont.). Booster inoculations were administered every 3 weeks, and anti-σNS titers were monitored by indirect enzyme-linked immunosorbent assay (ELISA) using MBP-σNS as an antigen (33). Once antibody titers were in excess of 1:1,000 by ELISA, mice were boosted with antigen in the absence of adjuvant, and spleens were harvested 3 days later. Spleen cells were mechanically dissociated and, using polyethylene glycol 4000 (Merck, Gibbstown, N.J.), fused

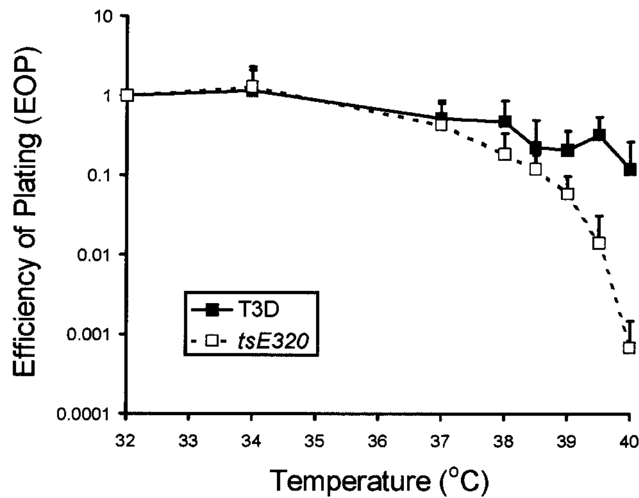

FIG. 2. EOP values for wt T3D and *tsE320*. EOP values were calculated by dividing the titer determined by plaque assay at each temperature by the titer determined at 32°C. The results are presented as the mean EOPs for at least six independent experiments. Error bars indicate standard deviations of the means.

with approximately 10^8 Sp2/0 myeloma cells. The products of each fusion were distributed into four 96-well plates (Costar, Cambridge, Mass.) containing murine peritoneal macrophage feeder layers. Cultures were incubated in HAT medium at 37°C for 10 to 14 days. When a majority of wells contained colonies that were 10 to 20% confluent, the supernatant from each well was screened for σNS antibodies by indirect ELISA using MBP-σNS as the antigen. Cells from antibody-positive wells were subcloned twice by limiting dilution in 96-well plates. Hybridoma cells secreting σNS antibodies (2×10^6) were injected into BALB/c mice intraperitoneally, and ascites fluid was harvested 7 to 9 days later. MAbs were purified on Econo-Pac protein A chromatography columns (Bio-Rad, Hercules, Calif.) and isotyped with a capture ELISA hybridoma subtyping kit (Roche).

Labeling of reovirus proteins with [^{35}S]methionine and [^{35}S]cysteine. L cells (5×10^6) in 25-cm^2 tissue culture flasks (Costar) were infected with reovirus strains at an MOI of 10 PFU per cell. Infected cells were incubated in methionine- and cysteine-free DMEM (Gibco) at either 32 or 39.5°C for 1 h before addition of radiolabel. One hundred microcuries of Translabel ([^{35}S]methionine and [^{35}S]cysteine) (NEN Life Science Products, Inc., Boston, Mass.) per ml in 3 ml of DMEM was added to each flask, and cells were incubated at either 32 or 39.5°C for 1 h. Cells were either harvested at the end of the labeling period or incubated in radiolabel-free medium at 32 or 39.5°C for additional intervals.

Immunoprecipitation of reovirus proteins. Cells containing radiolabeled reovirus proteins were lysed by incubation in 300 μl of lysis buffer (1% NP-40, 1% deoxycholate [DOC], 150 mM NaCl, 10 mM Tris [pH 7.4]) with 1% sodium dodecyl sulfate (SDS) and Complete EDTA-free protease inhibitor cocktail (Roche). Cell lysates were passed through a 25-gauge needle several times to shear the DNA and decrease the viscosity. Lysates were diluted eightfold in low-stringency immunoprecipitation buffer (1% NP-40, 1% DOC, 0.1% SDS, 150 mM NaCl, 10 mM Tris [pH 7.4]) and incubated in normal rabbit serum with protein A-Sepharose CL-4B beads (Amersham Pharmacia Biotech Inc., Piscataway, N.J.) at 4°C for 1 h. Protein A-Sepharose beads were collected by centrifugation at 250 × *g*, and the supernatant fractions were incubated with 10 μl of rabbit σNS-specific antiserum and protein A-Sepharose beads at 4°C overnight. Beads were collected by centrifugation and washed six times with high-stringency immunoprecipitation buffer (1% NP-40, 0.5% DOC, 0.1% SDS, 1 M NaCl, 10 mM Tris [pH 7.4]). Beads then were resuspended in 2× sample buffer (125 mM Tris, 10% β-mercaptoethanol, 4% SDS, 0.02% bromophenol blue) and incubated at 100°C for 5 min. Proteins were resolved by SDS-polyacrylamide gel electrophoresis (PAGE). Dried gels were exposed to an imaging plate, and band intensities were quantitated by determining photostimulus luminescence units with a Fuji2000 phosphorimager (Fuji Medical Systems, Inc., Stamford, Conn.). For each interval of incubation with radiolabel-free medium, the density of the band corresponding to the σNS protein was determined. Background density from lanes loaded with mock-infected cells was subtracted from the density of bands corresponding to σNS. Band density at each time point was divided by that at the 0-h time point and expressed as relative protein units.

TABLE 2. Genotypes, EOPs, and σNS subcellular localization of T1L × *tsE320* reassortant viruses

Virus strain	Parental origin of gene segment[a]:										EOP[b]	Subcellular localization of σNS[c]
	L1	L2	L3	M1	M2	M3	S1	S2	S3	S4		
Parental viruses												
T1L	1	1	1	1	1	1	1	1	1	1	0.50	Punctate
tsE320	E	E	E	E	E	E	E	E	E	E	0.00017	Diffuse
Reasortant viruses												
LE320.141	1	E	1	E	E	1	E	E	E	1	0.000007	Diffuse
LE320.29	E	E	E	E	E	E	1	E	E	1	0.000015	Diffuse
LE320.162	E	E	E	E	E	1	E	E	E	E	0.000045	Diffuse
LE320.106	E	E	E	E	E	E	1	E	E	E	0.000082	Diffuse
LE320.152	E	E	E	E	E	E	E	E	E	1	0.00011	Diffuse
LE320.104	1	E	E	E	E	E	E	E	E	1	0.00044	Diffuse
LE320.137	E	1	1	1	E	1	1	1	E	1	0.00049	Diffuse
LE320.129	1	E	E	E	E	E	E	E	E	E	0.0014	Diffuse
LE320.121	1	E	1	1	E	1	E	1	E	E	0.0016	Diffuse
LE320.114	1	E	1	E	E	E	E	1	E	1	0.0033	Diffuse
LE320.112	1	1	1	E	1	E	E	E	E	1	0.0072	Diffuse
LE320.66	1	1	1	1	1	E	1	1	1	1	0.056	Punctate
LE320.113	1	E	1	1	E	1	1	E	1	1	0.075	Punctate
LE320.32	1	1	1	1	E	1	1	1	1	1	0.083	Punctate
LE320.144	1	E	1	E	E	E	E	E	1	E	0.085	Punctate
LE320.164	E	1	E	E	E	E	1	E	1	1	0.16	Punctate
LE320.97	1	1	1	1	1	E	E	E	1	1	0.32	Punctate
LE320.158	E	E	E	E	E	E	E	E	1	E	0.33	Punctate
LE320.92	1	E	1	E	1	E	1	E	1	1	0.36	Punctate

[a] 1, T1L; E, *tsE320*.
[b] EOP is expressed as the titer at 39.5°C divided by the titer at 32°C. Reassortants were ranked from highest to lowest according to EOP to facilitate grouping.
[c] At a nonpermissive temperature of 39.5°C.

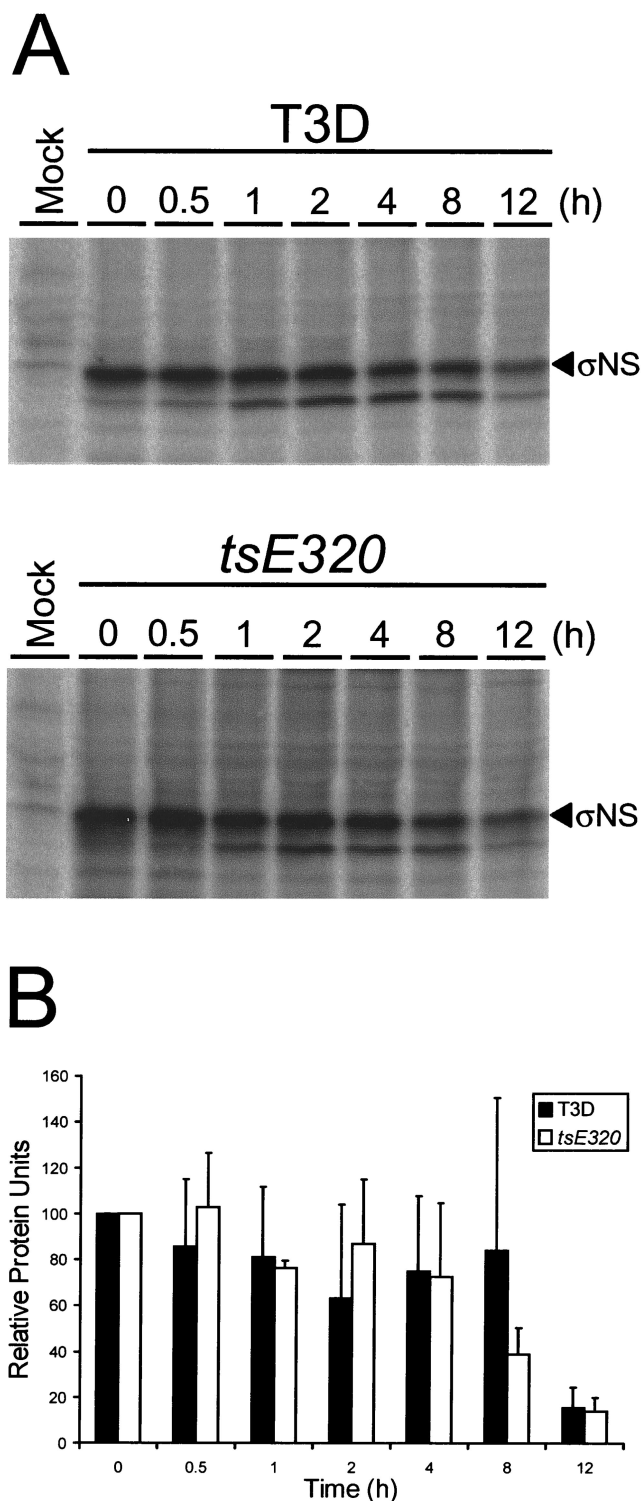

FIG. 3. Stability of reovirus σNS protein in cells infected with T3D or *tsE320* at a nonpermissive temperature. L cells were either mock infected or infected with either T3D or *tsE320* at an MOI of 10 PFU per cell and incubated at 39.5°C. At 6 h postinfection, cells were pulse-labeled with [^{35}S]methionine-[^{35}S]cysteine for 1 h and then incubated in the absence of radiolabeled methionine-cysteine for the time periods shown. The σNS protein was immunoprecipitated from cell lysates by using polyclonal σNS-specific antiserum, resolved by SDS-PAGE, visualized by autoradiography, and quantitated by phosphorimager analysis. (A) Representative autoradiogram. (B) Band densities corresponding to σNS protein, quantitated with a phosphorimager and normalized to the 0-h time point. The results are presented as the mean relative protein units for three independent experiments. Error bars indicate standard deviations of the means.

Immunofluorescence staining of reovirus-infected L cells. L cells (5×10^4 to 1×10^5) were grown on 12-mm-diameter glass coverslips (VWR Scientific Products, Atlanta, Ga.) for 24 to 48 h prior to infection with reovirus strains at an MOI of 10 PFU per cell. After adsorption at 4°C for 1 h, cells were incubated at 32, 37, or 39.5°C for various intervals, washed two times with phosphate-buffered saline (PBS), and fixed for 2 min in a 1:1 (vol/vol) mixture of methanol and acetone. Cells were kept in methanol at −20°C until stained. Cells were then washed two times in PBS and incubated for 15 min in PBS containing 5% γ-globulin-free bovine serum albumin (BSA; Sigma, St. Louis, Mo.). Nonspecific binding of antibody to cells was blocked by incubation for 10 min in PBS containing 1% BSA, 1% Triton X-100 (Bio-Rad), and 2% normal goat serum (Vector Laboratories, Inc., Burlingame, Calif.). Cells were incubated for 1 to 1.5 h with primary antibody at a concentration of 10 μg per ml (MAb 8H6 or 2H7) or a dilution of 1:500 (polyclonal T3D-, σNS-, or μ2-specific antiserum) and then washed two times. For double-staining experiments, the antibody chosen to detect σNS was determined by the nature of the antibody available to detect the other protein being examined. All washes and dilutions were done in PBS–BSA (1%)–Triton X-100 (1%)–normal goat serum (2%). Cells were then incubated with Alexa Fluor 488 or Alexa Fluor 546 goat anti-mouse immunoglobulin G (IgG) and Alexa Fluor 546 or Alexa Fluor 488 goat anti-rabbit IgG (Molecular Probes, Inc., Eugene, Oreg.) at a dilution of 1:1,000 for 1 to 1.5 h. Cells were washed two times for 15 min each time with PBS containing BSA (1%) and Triton X-100 (1%) and then two times for 10 min with PBS. Coverslips were washed with deionized water and then mounted on glass slides by using Aqua Poly/Mount (Polysciences, Inc., Warrington, Pa.) or ProLong Antifade (Molecular Probes). Cells were visualized using a Zeiss confocal fluorescence microscope (Carl Zeiss, New York, N.Y.). A differential interference contrast (DIC) image of each field of view was obtained to determine the location of cells. Coverslips containing mock-infected cells were included in every experiment and were processed along with infected cells. These cells were examined first and used to set the background on the confocal microscope to zero before obtaining images of infected cells. Images were processed and colored using Adobe Photoshop (Adobe Systems, Inc., San Jose, Calif.).

For direct immunofluorescence, IgG was isolated from polyclonal σNS- or μ2-specific antiserum using a protein A-Sepharose affinity column (Pierce, Rockford, Ill.). Eluted IgG was dialyzed exhaustively against PBS. The protein concentration of the IgG preparation was determined with the Bio-Rad protein assay. IgG was directly conjugated to either Alexa Fluor 488 or Alexa Fluor 546, using an Alexa Fluor 488 or Alexa Fluor 546 protein labeling kit (Molecular Probes). Cells were infected, fixed, hydrated, and blocked as described previously. Cells were incubated with a 1:250 dilution of the directly conjugated IgG for 1 to 1.5 h, washed and mounted as described previously, and then examined by confocal microscopy. Mock-infected cells were processed as described above and examined first to set the background fluorescence to zero before examination of infected cells. DIC images of each field of view were obtained. Images were processed and colored using Adobe Photoshop.

Electron microscopy. Thin-section electron microscopy of infected cells was performed as previously described (16) with minor modifications. L cells in suspension culture (2×10^7 per ml) were infected with reovirus strains at an MOI of 5 PFU per cell. After adsorption at 4°C for 1 h, cells were diluted to a density of 5×10^5 per ml in prewarmed, complete medium and incubated in suspension culture at either 32 or 39.5°C. Cells were prepared for thin-section electron microscopy by addition of freshly purified 50% aqueous glutaraldehyde (Electron Microscopy Sciences, Fort Washington, Pa.) directly to each sample (final concentration, 2%) and stored at 4°C. Fixed cells were washed three times in SC-Mg buffer (100 mM sodium cacodylate, 10 mM magnesium chloride), incubated for either 1 h in 1% osmium tetroxide in SC-Mg buffer or overnight in 2% uranyl acetate in SC-Mg buffer, washed two times in fresh SC-Mg buffer, and resuspended in an equal volume of 3% low-melting-point agarose. The agarose-cell molds were diced, dehydrated through a graded series of acetone immersions, and embedded in DER 332-732 (hard plastic composition) (Electron microscopy sciences). Ultrathin sections were prepared with a diamond knife (Microstar, Huntsville, Tex.) and an LKB Ultratome III ultramicrotome, mounted on 300-mesh copper hexagonal grids, and stained with 0.125% aqueous lead citrate in 0.1 M sodium hydroxide (41) followed by saturated ethanolic uranyl acetate (40). Sections were viewed at magnifications ranging from 4,500×

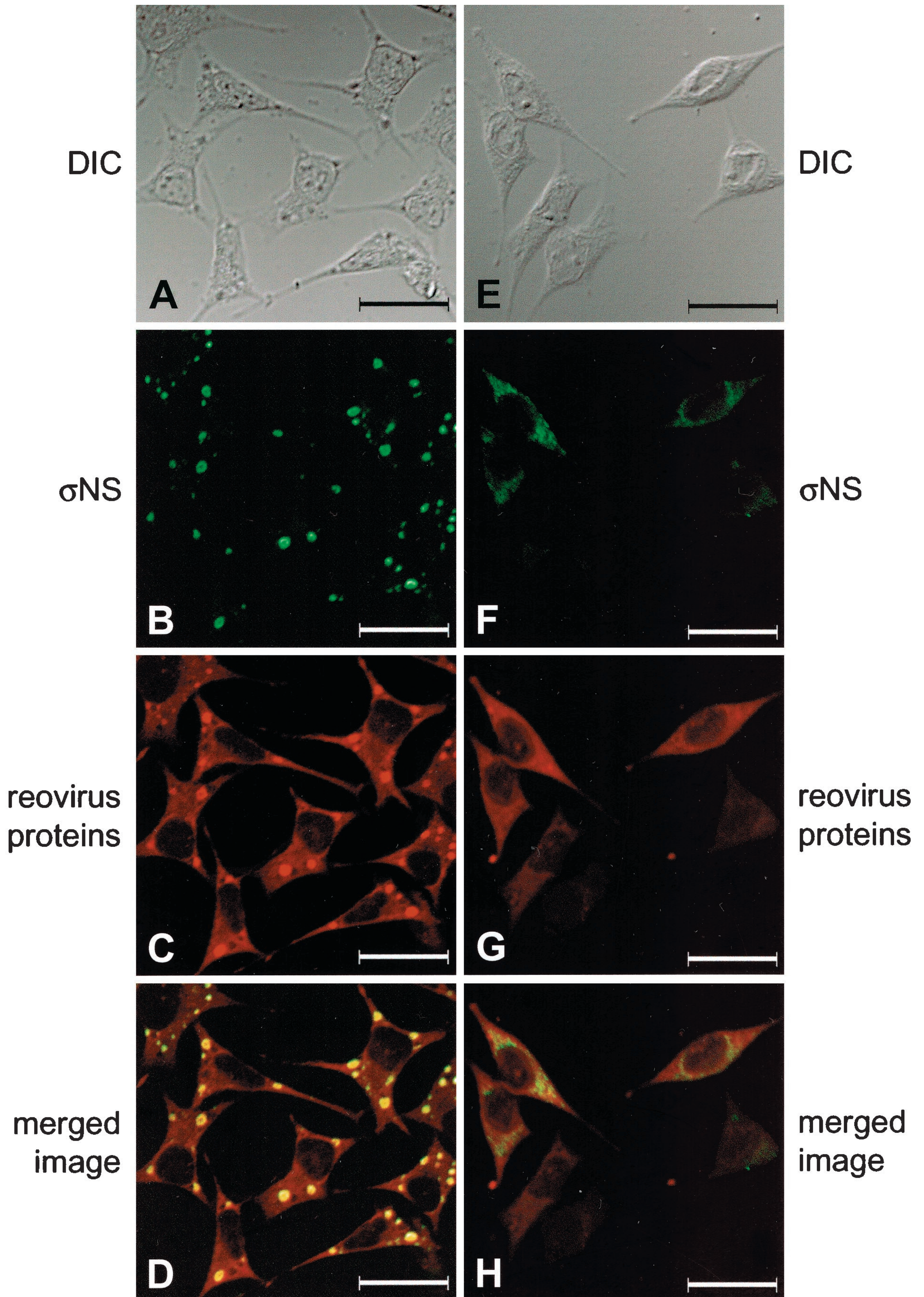

DIC
A
E
DIC
σNS
B
F
σNS
reovirus proteins
C
G
reovirus proteins
merged image
D
H
merged image

to 100,000× in a Phillips model 201 electron microscope at an acceleration voltage of 60 keV. Specimen images were recorded on Kodak Direct Positive film 5302, and electron micrographs were printed on Kodak Polycontrast III paper.

Nucleotide sequence accession number. The nucleotide sequence of the σNS ORF of the laboratory clone of *tsE320* was submitted to GenBank and assigned accession no. AF076293.

RESULTS

The reovirus σNS protein localizes to sites of viral assembly. To determine the subcellular localization of nonstructural protein σNS, we used confocal immunofluorescence microscopy to examine mouse L cells infected with wt reovirus strain T3D. To facilitate these experiments, we cloned and expressed the reovirus σNS protein with either a carboxy-terminal six-histidine tag or an amino-terminal MBP tag. The expressed proteins were used to generate a σNS-specific polyclonal antiserum and a new panel of σNS-specific MAbs (Table 1). L cells were infected with T3D, stained with σNS-specific antiserum, and examined by confocal fluorescence microscopy (Fig. 1). The σNS protein localized to discrete, punctate sites, usually in a perinuclear location. The patterns of σNS localization when using either polyclonal antiserum or MAbs were identical (data not shown). To determine whether σNS localizes to sites of viral assembly, T3D-infected cells were stained with a σNS-specific polyclonal antiserum (Fig. 1B) and μ1/μ1C-specific MAb 8H6 (42) (Fig. 1C). Reovirus μ1/μ1C protein is an outer-capsid protein added to virions after cores are assembled (22, 50). Detection of μ1/μ1C by immunofluorescence staining has been used previously to indicate the presence of viral inclusions (34). The σNS protein and the μ1/μ1C protein colocalized to distinct perinuclear sites in infected cells (Fig. 1D), indicating that σNS localizes to sites of viral assembly.

Characterization of *tsE320*. To determine the role of σNS in formation of inclusions in reovirus-infected cells, we examined cells infected with mutant virus *tsE320*. The *tsE320* clone used in this study exhibited temperature sensitivity at all temperatures tested above 39°C (Fig. 2). Therefore, in subsequent experiments, a nonpermissive temperature of 39.5°C was used. The *ts* defect in *tsE320* had been mapped previously to the S3 gene by reassortant analysis (30). To confirm that the *ts* phenotype of our clone segregates with the S3 gene, we isolated new T1L × *tsE320* reassortant viruses and determined efficiency of plating (EOP) values at 39.5°C for the parental and reassortant viruses (Table 2). Reassortant viruses containing an S3 gene from *tsE320* had EOP values of less than 0.01, whereas those with an S3 gene from T1L had EOP values of greater than 0.05. No other gene segments were found to segregate with the differences in EOP values exhibited by the T1L × *tsE320* reassortant viruses. These results confirm that a *ts* defect in S3 gene product σNS is responsible for impaired growth of *tsE320* at a nonpermissive temperature.

To test whether the mutation in *tsE320* σNS alters the stability of the protein, pulse-chase experiments were performed. L cells were infected at 39.5°C with either T3D or *tsE320* and, at 6 h postinfection, incubated with medium containing [^{35}S]methionine-[^{35}S]cysteine for 1 h. After the labeling period, cells were incubated in the absence of radiolabel for various intervals, and σNS protein was immunoprecipitated with polyclonal σNS-specific antiserum and resolved by SDS-PAGE (Fig. 3A). The intensities of bands corresponding to the T3D and *tsE320* σNS proteins were quantitated by phosphorimager analysis and normalized to the 0-h time point (Fig. 3B). The relative band intensities of the T3D and *tsE320* σNS proteins were found to be equivalent over a 12-h time course, indicating that these proteins do not differ in stability at a nonpermissive temperature. Therefore, the temperature-dependent phenotypes attributable to *tsE320* σNS are not likely to result from premature protein degradation.

The nucleotide sequence of the σNS ORF of the laboratory clone of *tsE320* was determined. U-to-C nucleotide substitutions were found at positions 806 and 1057. The first results in a methionine-to-threonine substitution at amino acid 260 and has been previously reported (45); the second is a silent mutation. These results show that the *tsE320* laboratory clone contains the mutation previously identified in the S3 gene.

The σNS protein is required for viral inclusion formation. To determine whether σNS is required for formation of reovirus assembly complexes, we examined the subcellular localization of σNS in cells infected with either wt T3D or *tsE320*. Infected cells were fixed 24 h after adsorption, stained with σNS-specific MAb 2H7 and polyclonal T3D-specific antiserum, and imaged by confocal fluorescence microscopy. In cells infected with wt T3D, the σNS protein localized to punctate, perinuclear structures (Fig. 4B). Reovirus proteins were distributed throughout the cytoplasm and also concentrated in discrete perinuclear foci (Fig. 4C). When these images were merged, σNS colocalized with other reovirus proteins, confirming that σNS localizes to areas of progeny virion assembly in viral inclusions (Fig. 4D). Identical staining patterns were observed for T3D-infected cells incubated at 32, 37, or 39.5°C and for *tsE320*-infected cells incubated at 32 or 37°C, the only difference being an increase in the rate of inclusion formation at higher temperatures (data not shown). However, in cells infected with *tsE320* at 39.5°C, σNS was distributed throughout the cytoplasm and exhibited a granular staining pattern not seen in cells infected with wt reovirus (Fig. 4F). Reovirus proteins were distributed diffusely in the cytoplasm of cells infected with *tsE320* at 39.5°C, and inclusion structures were not observed (Fig. 4G). When cells were incubated for periods up to 96 h at a nonpermissive temperature, approximately 50% of the *tsE320*-infected cells contained demonstrable σNS; however, staining was diffuse and granular (data not shown). When images of σNS and other reovirus proteins were merged, only

FIG. 4. Subcellular localization of σNS and reovirus proteins in cells infected with wt T3D or mutant *tsE320* at a nonpermissive temperature. L cells were infected with either T3D (A to D) or *tsE320* (E to H) at an MOI of 10 PFU per cell and incubated at 37°C (T3D) or 39.5°C (*tsE320*) for 24 h. Cells were stained for σNS by using σNS-specific MAb 2H7 (B and F) and for reovirus proteins by using a polyclonal antiserum raised against T3D (C and G) as primary antibodies followed by Alexa Fluor 488 goat anti-mouse IgG and Alexa Fluor 546 goat anti-rabbit IgG, respectively, as secondary antibodies. Images were obtained by using a confocal microscope. The σNS protein is colored green, and the reovirus proteins are colored red. (A and E) A DIC image of each field was obtained. (D and H) In the merged images, colocalization of σNS and reovirus proteins is indicated by the yellow color. Images were processed using Adobe Photoshop. Bars, 25 μm.

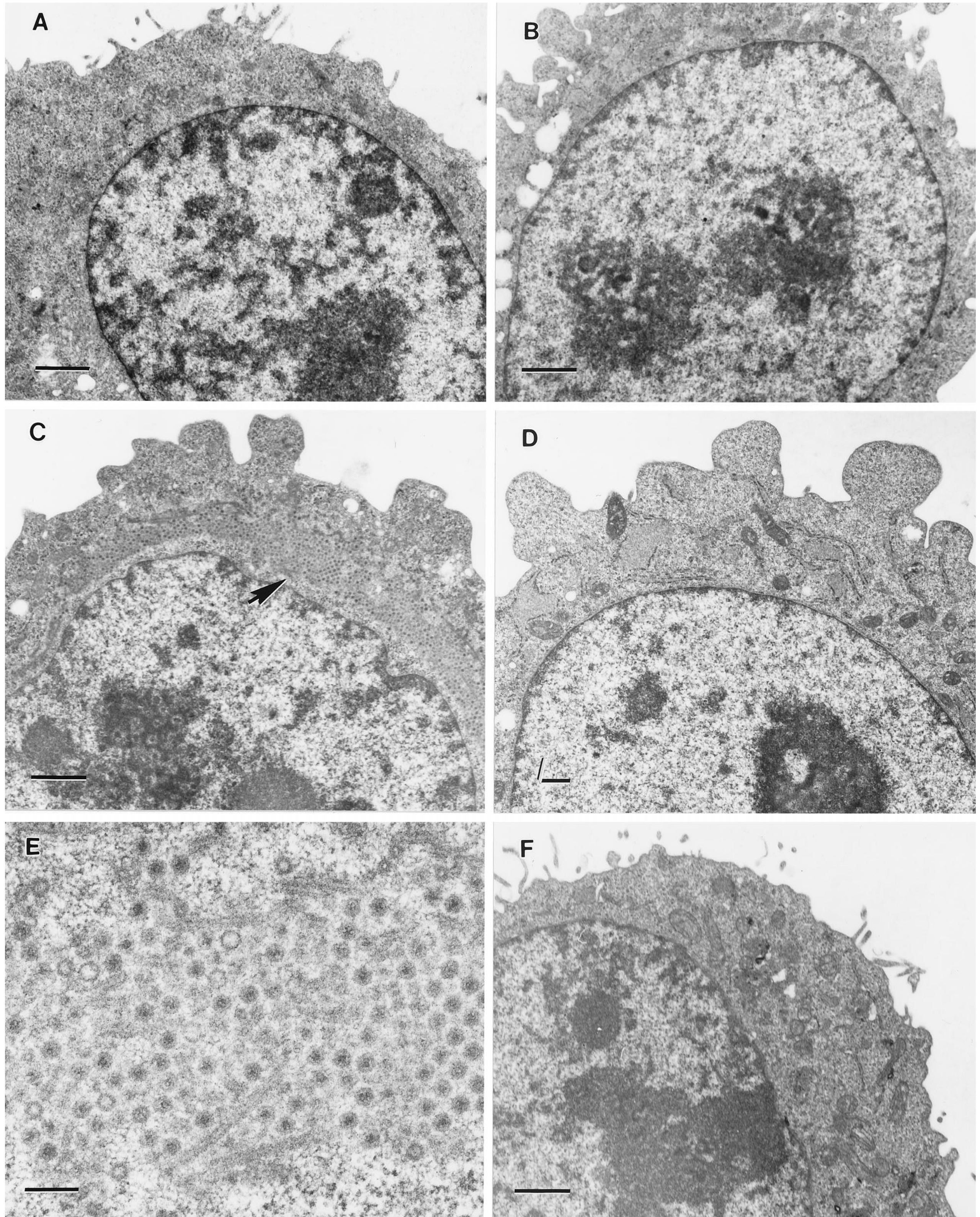

FIG. 5. Ultrastructural analysis of cells infected with *tsE320* at permissive and nonpermissive temperatures. L cells were infected with *tsE320* at an MOI of 5 PFU per cell and incubated at either 32°C (A, C, and E) or 39.5°C (B and D). Cells were harvested at 12 (A) or 36 (C and E) h postinfection for cultures incubated at 32°C and at 8 (B) or 24 (D) h postinfection for cultures incubated at 39.5°C. Cells were fixed with glutaraldehyde, embedded, sectioned, stained, and examined with a Phillips 201 electron microscope. (E) A higher magnification of the area demarcated by an arrow in panel C. (F) Mock-infected L cells incubated at 39.5°C for 24 h and processed according to the protocol used for infected cells. Bars, 1 μm (A to D and F) and 200 nm (E).

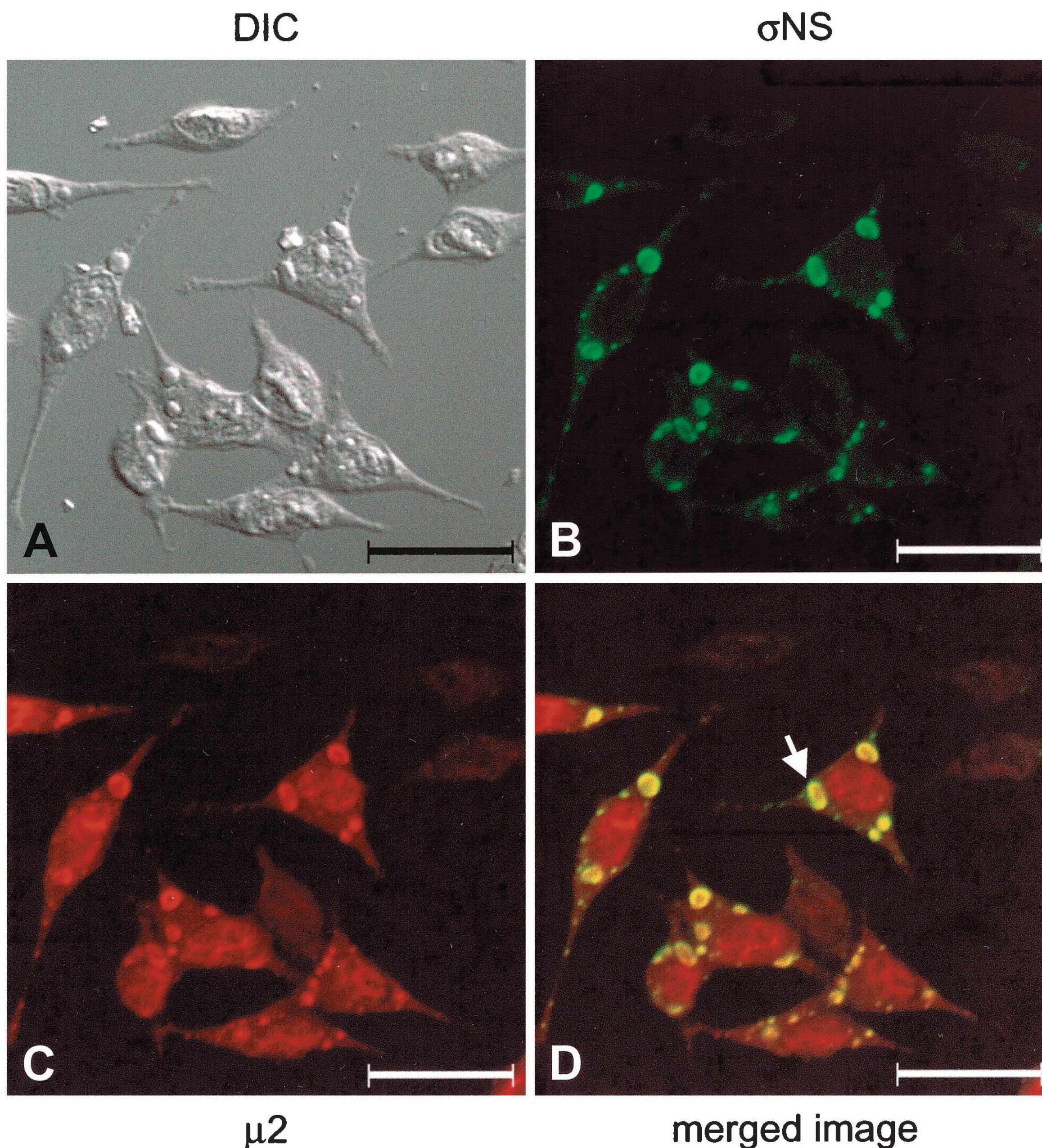

FIG. 6. Subcellular localization of reovirus σNS and μ2 proteins in cells infected with reovirus strain T3D. L cells were infected with T3D at an MOI of 10 PFU per cell and incubated at 37°C for 18 h. Cells were stained for σNS by using σNS-specific MAb 2H7 (B) and for μ2 by using a μ2-specific polyclonal antiserum (C) as primary antibodies followed by Alexa Fluor 546 goat anti-mouse IgG and Alexa Fluor 488 goat anti-rabbit IgG, respectively, as secondary antibodies. Images were obtained by using a confocal microscope. The σNS protein is colored green, and the μ2 protein is colored red. (A) A DIC image of the field was obtained. (D) In the merged image, colocalization of σNS and μ2 is indicated by the yellow color. The arrow indicates a viral inclusion in which three different zones of viral proteins are evident: a red (μ2) center, a yellow (σNS and μ2) intermediate zone, and a narrow peripheral zone of green (σNS). Images were processed using Adobe Photoshop. Bars, 25 μm.

a small amount of yellow color was seen, indicating minimal colocalization of σNS with other reovirus proteins (Fig. 4H). These results suggest that σNS localizes to viral inclusions and that functional σNS is required for the formation of these structures.

To confirm these findings, we used electron microscopy to visualize intracellular sites of viral assembly. Suspension cultures of L cells were infected with either T3D or *tsE320* and examined by thin-section electron microscopy (Fig. 5). At a permissive temperature, cells infected with either T3D or *tsE320* demonstrated formation of viral inclusions with similar kinetics. The first small inclusions in cells infected with either strain were detectable 18 h postinfection (Figs. 5A and C and data not shown). By 36 h postinfection, these foci of viral infection had developed into well-defined cytoplasmic inclusions that displaced the nucleus eccentrically (Fig. 5C). By 72 h

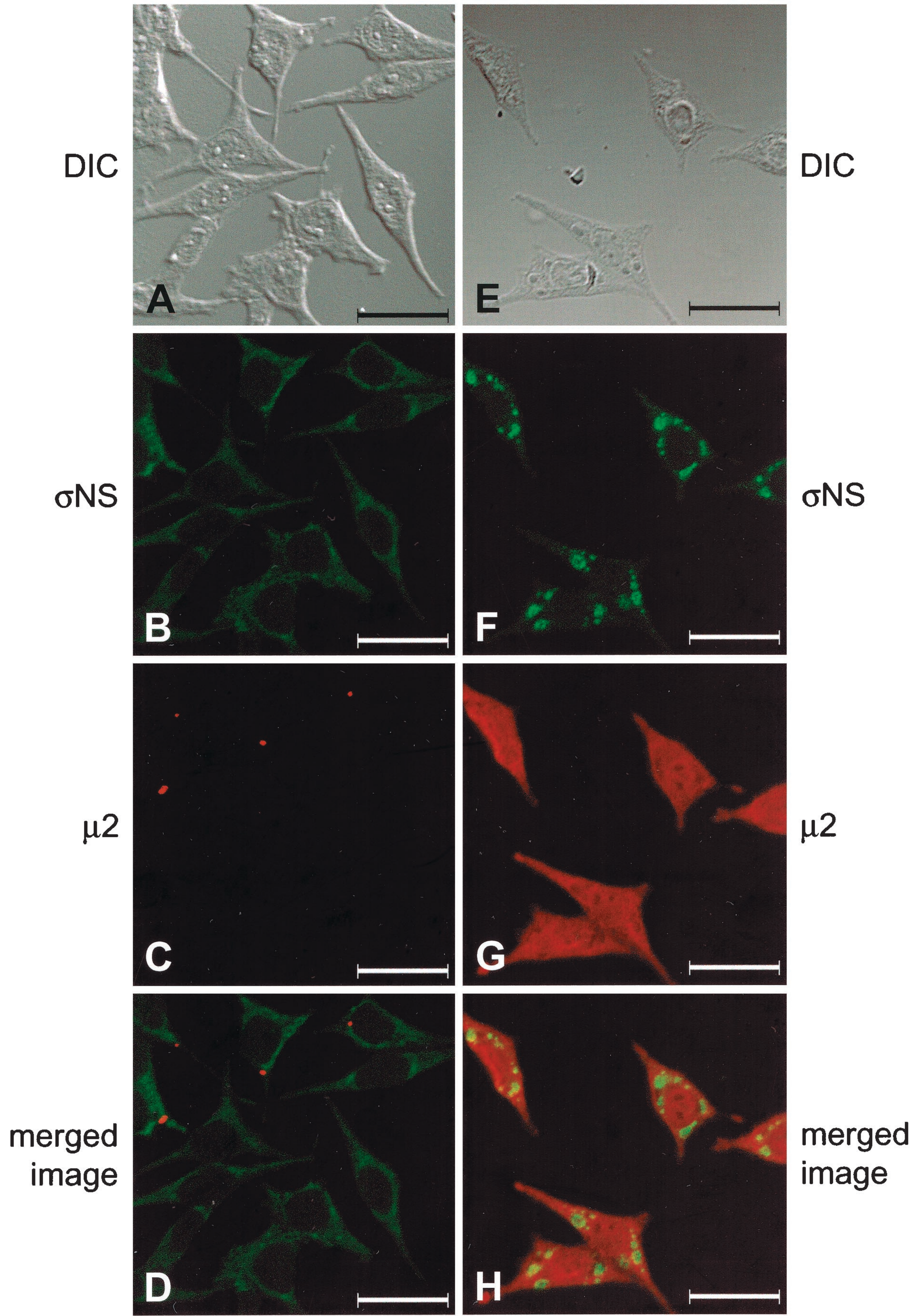
DIC
σNS
μ2
merged
image
A
B
C
D
E
F
G
H

postinfection, every cell examined demonstrated evidence of viral infection (data not shown). Later in the course of infection, paracrystalline arrays of assembling virions associated with cytoskeletal elements were apparent (Fig. 5E). Cells infected with *tsE320* at a nonpermissive temperature remained morphologically unchanged for the duration of observation and did not demonstrate evidence of viral infection at any time point examined (Figs. 5B and D), up to and including 72 h postinfection (data not shown).

To rigorously determine the requirement of σNS for formation of viral inclusions, we examined the capacity of T1L × *tsE320* reassortant viruses to form inclusions at a nonpermissive temperature. L cells were infected with T1L, *tsE320*, or one of 19 T1L × *tsE320* reassortant viruses and incubated at either 31 or 39.5°C for 24 h, stained with σNS-specific MAb 2H7, and examined by fluorescence microscopy (Table 2). At 31°C, each parental and reassortant virus produced perinuclear inclusions that contained σNS (data not shown). However, at 39.5°C, only virus strains containing a T1L S3 gene showed σNS-positive perinuclear inclusions; those containing a *tsE320* S3 gene exhibited diffuse cytoplasmic staining for σNS. Therefore, the capacity to form viral inclusions in reovirus-infected cells segregates with the σNS-encoding S3 gene, indicating that functional σNS is required for viral inclusion formation.

Reovirus σNS but not μ2 is required for formation of inclusion-like structures. In a previous study, we found that strain-specific differences in the rate of viral inclusion formation segregate with the μ2-encoding M1 gene, with a secondary contribution attributed to the σNS-encoding S3 gene (19). To determine the requirement of μ2 for the formation of viral inclusions and the relationship of σNS and μ2 in this process, we examined the subcellular localization of σNS and μ2 during the course of reovirus infection. L cells were infected with wt T3D, stained with σNS-specific MAb 2H7 and polyclonal μ2-specific antiserum (19), and imaged by confocal fluorescence microscopy (Fig. 6). The σNS protein was found in discrete, perinuclear structures within the cytoplasm (Fig. 6B), as observed previously (Fig. 1B and 4B). The μ2 protein was distributed diffusely in both the cytoplasm and the nucleus (19) and also was concentrated in discrete, perinuclear structures (Fig. 6C). When these images were merged, the σNS protein colocalized with foci of concentrated μ2 protein (Fig. 6D), indicating that both proteins were present at the same perinuclear sites, which correspond to viral inclusions. In larger inclusions, zones of green (σNS), yellow (σNS and μ2), and red (μ2) were seen progressively from the periphery to the center of the inclusion structure (Fig. 6D). This pattern of protein staining was similar to that seen when T3D-infected cells were examined for the subcellular localization of σNS and μ1/μ1C (Fig. 1). In immunoelectron microscopy experiments using gold-conjugated polyclonal σNS-specific antiserum, most of the gold beads were present near the periphery of the inclusions (data not shown), which is consistent with the findings obtained by confocal immunofluorescence microscopy. These observations suggest that σNS exists at the periphery of mature inclusions whereas μ2 has a more central location in these structures.

We next examined the subcellular localization of σNS and μ2 in cells infected with either *tsE320* or *tsH11.2* at a nonpermissive temperature. Infected cells were stained with σNS-specific MAb 2H7 and polyclonal μ2-specific antiserum and imaged by confocal fluorescence microscopy. In cells infected with *tsE320*, σNS exhibited a diffuse, granular staining pattern within the cytoplasm (Fig. 7B), as observed previously (Fig. 4F), whereas μ2 formed small, punctate structures within the cytoplasm (Fig. 7C). The two proteins were not observed to colocalize, as indicated by the absence of yellow color in the merged image (Fig. 7D). In cells infected with *tsH11.2*, μ2 was distributed diffusely in both the cytoplasm and the nucleus and did not form inclusion-like structures (Fig. 7G). In sharp contrast, σNS was found in discrete, punctate structures and demonstrated a staining pattern indistinguishable from that seen in cells infected with wt reovirus (Fig. 7F). However, when these images were merged, σNS and μ2 did not colocalize, again indicated by the absence of yellow color (Fig. 7H). To determine whether the σNS- or μ2-containing complexes included other reovirus proteins, the subcellular localization of μ1/μ1C in combination with either μ2 or σNS was examined in cells infected with either *tsE320* or *tsH11.2*. In cells infected with *tsE320*, μ2 was observed in small, punctate structures within the cytoplasm (Fig. 8B). No μ1/μ1C was detected in *tsE320*-infected cells (Fig. 8C), even when cells were examined at 36 or 48 h postinfection (data not shown). In cells infected with *tsH11.2*, σNS was found in discrete, punctate structures within the cytoplasm (Fig. 8F) and μ1/μ1C exhibited a similar staining pattern (Fig. 8G). When these images were merged, σNS and μ1/μ1C colocalized, as indicated by the yellow color (Fig. 8H). Therefore, the μ2-containing structures seen in *tsE320*-infected cells do not resemble viral inclusions in terms of size, location, or protein composition, while the σNS-containing structures seen in *tsH11.2*-infected cells resemble viral inclusions observed in cells infected with wt reovirus. These results suggest that the block to viral replication exhibited by *tsE320* occurs at a point in the replication cycle prior to that exhibited by *tsH11.2*.

The σNS protein precedes the μ2 protein in localization to viral inclusions. Results gathered thus far are consistent with the hypothesis that σNS is required for nucleation of sites of viral replication to which other viral proteins, including μ2, are recruited. To determine whether σNS localizes to discrete structures in reovirus-infected cells prior to localization of μ2 to these structures, we examined cells infected with wt reovirus

FIG. 7. Subcellular localization of reovirus σNS and μ2 proteins in cells infected with mutant strains *tsE320* and *tsH11.2*. L cells were infected with either *tsE320* (A to D) or *tsH11.2* (E to H) at an MOI of 10 PFU per cell and incubated at 39.5°C for either 12 (*tsH11.2*) or 24 (*tsE320*) h. Cells were stained for σNS by using σNS-specific MAb 2H7 (B and F) and for μ2 by using a μ2-specific polyclonal antiserum (C and G) as primary antibodies followed by Alexa Fluor 488 goat anti-mouse IgG and Alexa Fluor 546 goat anti-rabbit IgG, respectively, as secondary antibodies. Images were obtained by using a confocal microscope. The σNS protein is colored green, and the μ2 protein is colored red. (A and E) A DIC image of each field was obtained. (D and H) In the merged images, lack of colocalization of σNS and μ2 is indicated by the lack of yellow color. Images were processed using Adobe Photoshop. Bars, 25 μm.

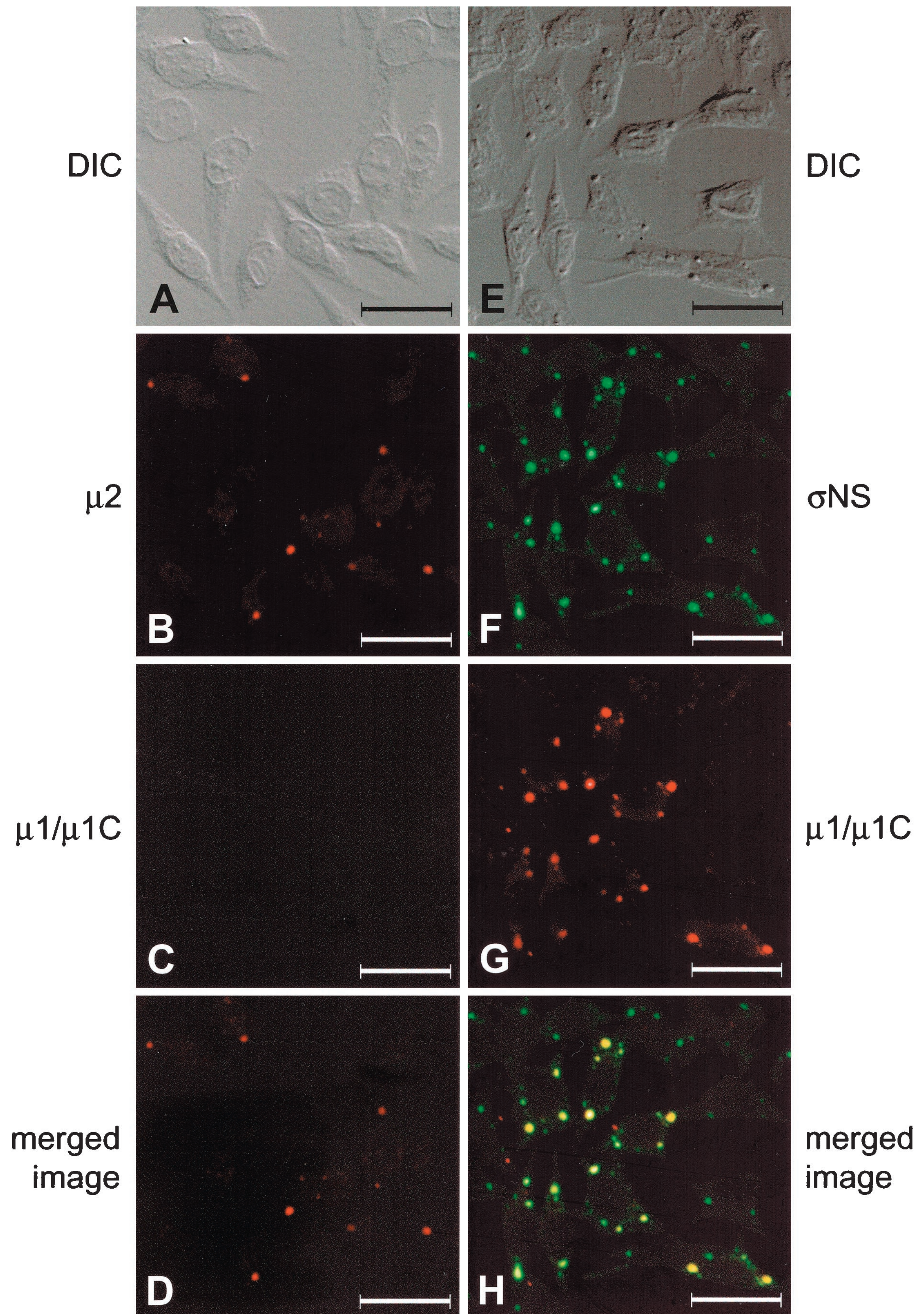
DIC
μ2
μ1/μ1C
merged image
A
B
C
D
DIC
σNS
μ1/μ1C
merged image
E
F
G
H

over a time course of infection. To minimize potential differences in avidity of MAbs and polyclonal antiserum, we purified IgG from polyclonal σNS- and μ2-specific antisera and directly conjugated each to different fluorophores. L cells were infected with wt T3D, fixed at 2-h intervals, stained with the conjugated σNS- and μ2-specific antisera, and imaged by confocal microscopy (Fig. 9). The σNS protein was first detected at 8 h postinfection and was distributed diffusely in the cytoplasm. By 10 h postinfection, σNS was observed in small, punctate structures throughout the cytoplasm and μ2 was distributed diffusely. By 14 h postinfection, μ2 was observed to colocalize with a subset of the σNS-containing structures. Between 14 and 18 h, structures containing both σNS and μ2 increased in size and grew to resemble mature viral inclusions. At later time points of infection, larger inclusions were observed, with σNS concentrating at the periphery and μ2 concentrating in the center. These results indicate that σNS forms protein complexes prior to μ2 and support the hypothesis that σNS-containing complexes nucleate formation of viral inclusions.

DISCUSSION

Reovirus σNS-mutant *tsE320* has been reported to have a defect in synthesis of viral dsRNA (8, 9). We hypothesized that the defect exhibited by *tsE320* affects either assembly of protein-RNA complexes prior to dsRNA synthesis or the capacity of the viral polymerase to complete dsRNA synthesis following protein complex formation. Our results indicate that functional σNS is required for the formation of viral assembly complexes and suggest that σNS recruits other proteins to intracellular sites of viral assembly.

In reovirus-infected cells, the σNS protein localizes primarily to discrete perinuclear sites within the cytoplasm. Other reovirus proteins are also found in these structures, indicating that the σNS-containing protein complexes correspond to viral inclusions observed by electron microscopy (11). In contrast to cells infected with wt reovirus, viral inclusions are not detectable in cells infected with *tsE320* at a nonpermissive temperature. This finding suggests that σNS is required for viral inclusion formation, a conclusion strengthened by analysis of T1L × *tsE320* reassortant viruses. Cells infected with reassortant viruses containing a wt T1L S3 gene formed σNS-positive inclusions, whereas cells infected with reassortant viruses containing a *tsE320* S3 gene exhibited a diffuse staining pattern for σNS. These data provide strong evidence that reovirus inclusion formation requires functional σNS.

Viral inclusion formation in *tsE320*-infected cells at a nonpermissive temperature was markedly diminished but not completely abolished. Less than 5% of cells infected with *tsE320* at 39.5°C contained viral inclusions (data not shown), which is consistent with an EOP for *tsE320* at 39.5°C of 1.4×10^{-2}. The restriction to formation of viral inclusions in cells infected with *tsE320* was not simply due to a temperature-dependent instability of σNS. By pulse-chase analysis, the stabilities of T3D and *tsE320* σNS proteins at a nonpermissive temperature were equivalent over a 12-h period of observation. In addition, when cells infected with *tsE320* were incubated at a nonpermissive temperature for intervals of up to 96 h prior to examination, the diffuse staining pattern for σNS was maintained (data not shown). These results demonstrate that the mutation in *tsE320* σNS alters its capacity to form assembly complexes rather than its stability.

In addition to σNS, viral core protein μ2 also plays a role in formation of viral inclusions (19). The rates of viral inclusion formation of reovirus strains T1L and T3D differ; the median times of inclusion formation are 39 h in cells infected with T1L and 18 h in cells infected with T3D. Using T1L × T3D reassortant viruses, the μ2-encoding M1 gene was found to segregate with this strain-specific difference in kinetics of viral inclusion formation (19). Interestingly, in reassortant viruses containing a T3D M1 gene, the σNS-encoding S3 gene also was found to segregate with differences in kinetics of inclusion formation. Reovirus mutant *tsH11.2* contains a lesion in the μ2-encoding M1 gene (4) and, like *tsE320*, does not complete dsRNA synthesis at a nonpermissive temperature (4). Cells infected with *tsH11.2* at a nonpermissive temperature formed structures that contain σNS and outer-capsid protein μ1/μ1C and morphologically resemble viral inclusions seen in cells infected with wt reovirus. The μ2 protein appeared to be excluded from these inclusion-like structures, which suggests that functional μ2 is not required for viral assembly complex formation. The inclusion-like structures present in *tsH11.2*-infected cells at a nonpermissive temperature do not form virions (4) and thus are clearly not mature viral inclusions. It is possible that the structures observed in *tsH11.2*-infected cells are early assembly complexes nucleated by σNS that fail to mature into viral inclusions due to the lack of dsRNA synthesis resulting from the absence of functional μ2. This hypothesis is consistent with a proposed role for μ2 in viral polymerase activity (26, 46).

A qualitative difference in the amounts of protein produced in cells infected with T3D or *tsE320* at a nonpermissive temperature was noted in this study. These viruses produced approximately equivalent amounts of protein early in infection, as detected by pulse-chase analysis of σNS (Fig. 3) and immunoprecipitation of other reovirus proteins (data not shown). However, at late time points of infection, there appeared to be much more viral protein in cells infected with either T3D or

FIG. 8. Subcellular localization of reovirus proteins in cells infected with mutant strains *tsE320* and *tsH11.2*. L cells were infected with either *tsE320* (A to D) or *tsH11.2* (E to H) at an MOI of 10 PFU per cell and incubated at 39.5°C for either 18 (*tsH11.2*) or 24 (*tsE320*) h. Cells infected with *tsE320* were stained for μ2 by using a μ2-specific polyclonal antiserum (B) and for μ1/μ1C by using μ1/μ1C-specific MAb 8H6 (C) as primary antibodies followed by Alexa Fluor 546 goat anti-rabbit IgG and Alexa Fluor 488 goat anti-mouse IgG, respectively, as secondary antibodies. Cells infected with *tsH11.2* were stained for σNS by using a σNS-specific polyclonal antiserum (F) and for μ1/μ1C by using μ1/μ1C-specific MAb 8H6 (G) as primary antibodies followed by Alexa Fluor 546 goat anti-rabbit IgG and Alexa Fluor 488 goat anti-mouse IgG, respectively, as secondary antibodies. Images were obtained by using a confocal microscope. In images of cells infected with *tsE320*, the μ2 protein is colored red and the μ1/μ1C protein is colored green. In images of cells infected with *tsH11.2*, the σNS protein is colored green and the μ1/μ1C protein is colored red. (A and E) A DIC image of each field was obtained. (D and H) In the merged images, colocalization of the proteins is indicated by the yellow color. Images were processed using Adobe Photoshop. Bars, 25 μm.

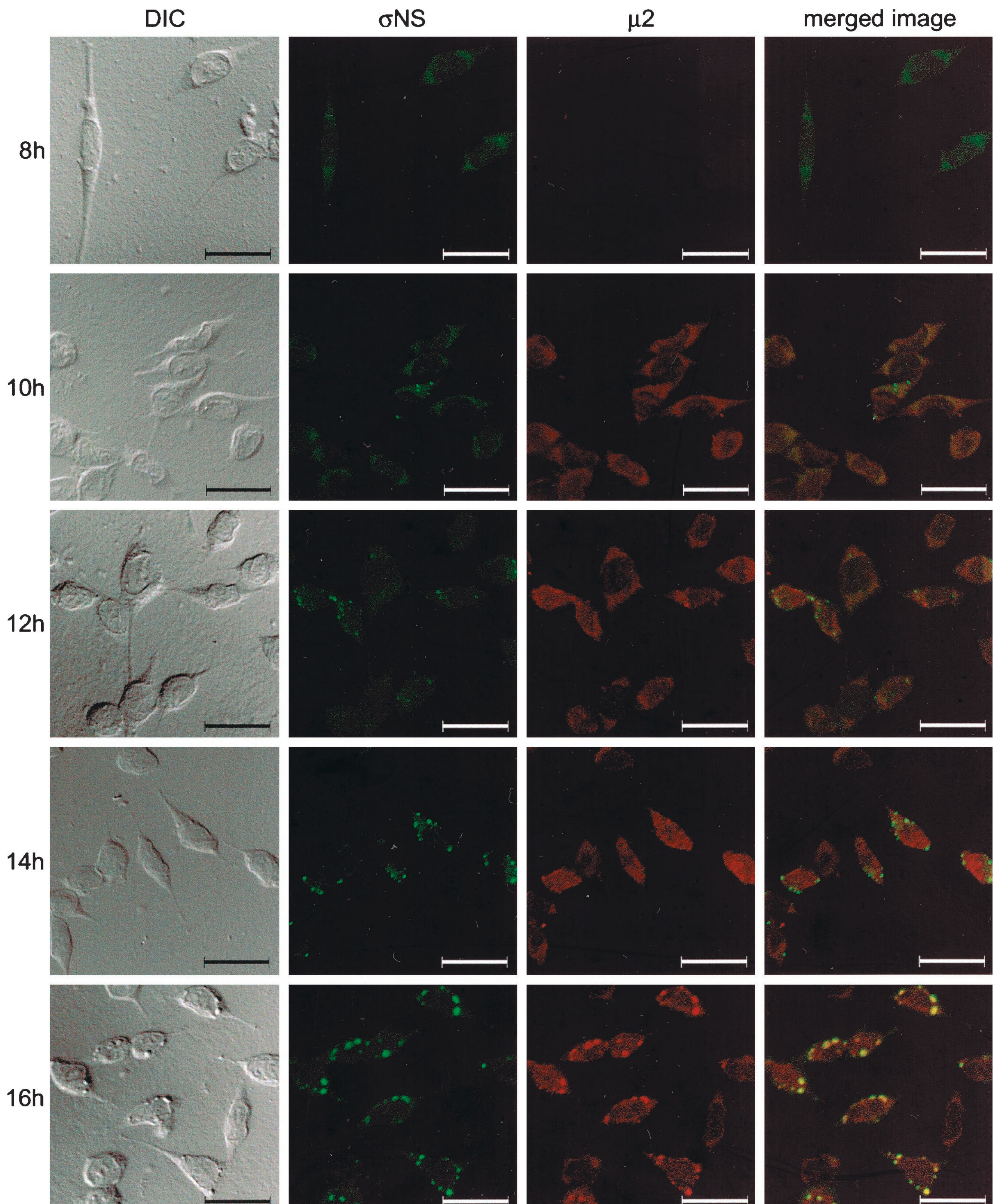

FIG. 9. Subcellular localization of σNS and μ2 proteins in cells infected with T3D, determined at different times postinfection. L cells were infected with T3D at an MOI of 10 PFU per cell and incubated at 37°C for the time periods shown. Cells were stained for σNS by using a σNS-specific polyclonal antiserum directly conjugated to Alexa Fluor 546 and for μ2 by using a μ2-specific polyclonal antiserum directly conjugated to Alexa Fluor 488. Images were obtained by using a confocal microscope. The σNS protein is colored green, and the μ2 protein is colored red. A DIC image of each field was obtained. In the merged image, colocalization of σNS and μ2 is indicated by the yellow color. Images were processed using Adobe Photoshop. Bars, 25 μm.

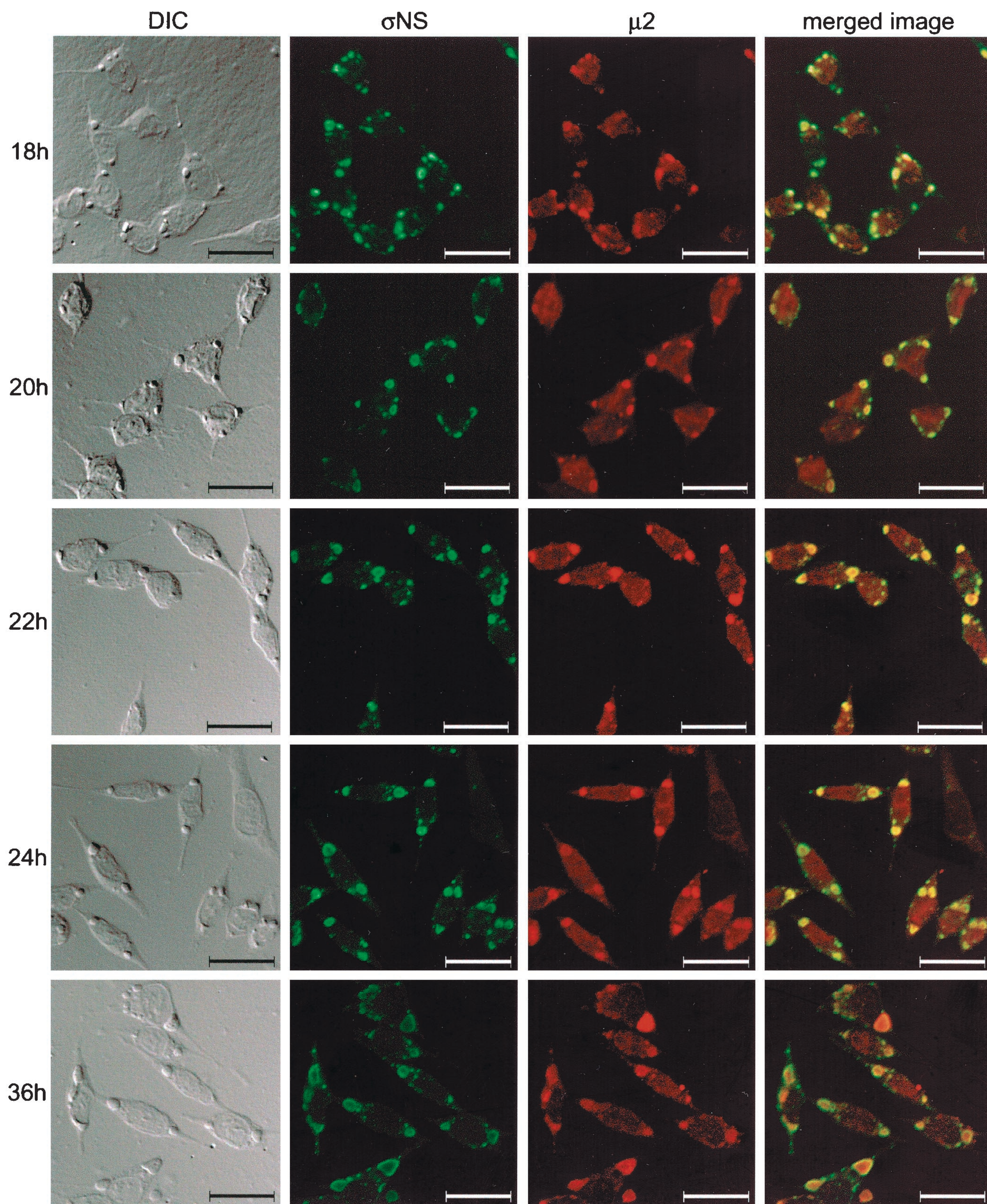

FIG. 9—*Continued.*

tsH11.2 than in those infected with *tsE320*, as judged by confocal immunofluorescence microscopy. This effect was not confined to σNS, since cells infected with *tsE320* also produced less μ1/μ1C and μ2 than cells infected with either T3D or *tsH11.2*. It is possible that the effects of σNS on viral protein synthesis are due to direct interactions of σNS with the translational machinery, as has been reported for rotavirus nonstructural protein NSP3 (27), or occur as a consequence of the function of σNS in formation of viral assembly complexes.

To determine more precisely the roles of σNS and μ2 in viral inclusion formation, we examined the subcellular localization of both proteins in reovirus-infected cells by confocal immunofluorescence microscopy at different time points postinfection. We found that σNS localizes to punctate structures in the cytoplasm prior to μ2. By 14 h postinfection, both σNS and μ2 are found in discrete, punctate structures, which then decrease in number, increase in size, and coalesce at perinuclear sites. At all time points examined, the smallest of the σNS-containing complexes do not include μ2. The μ1/μ1C protein is also undetectable in the smallest σNS-containing structures (data not shown), which suggests that σNS is found at sites of viral assembly prior to either μ2 or μ1/μ1C. Larger structures stain positively for both σNS and μ2; however, at late time points of infection, σNS appears to be excluded from the center of the larger inclusions while μ2 is present throughout these structures. It is likely that the central region of enlarging inclusions contains progeny virions and a full complement of viral structural proteins, including μ2. It is possible that an intermediate zone of the inclusions, which contains both σNS and μ2, represents the location of ongoing viral assembly and that the outermost rim of the inclusions, in which σNS but not μ2 resides, represents the site at which σNS is actively recruiting other viral proteins. This model of reovirus assembly suggests that as viral inclusions mature, σNS moves to the periphery as it facilitates recruitment of viral structural proteins to be used in assembly of additional progeny virions. Since it has been determined by electron microscopy that ribosomes are present at the periphery of viral inclusions (47), it is also possible that viral proteins in the inclusion structure originate from enhanced local protein synthesis, which might be influenced by σNS. As an alternative explanation for our findings, it is possible that once outer-capsid proteins are added to maturing virions, the protein components of the viral core, including μ2, are inaccessible to antibodies for immunofluorescence staining. Thus, the outer zone of the inclusion structures in which σNS is present and μ2 is absent might represent the presence of mature virions surrounded by nonstructural protein σNS. However, since the majority of mature double-shelled particles, as observed by electron microscopy, are in the center of the inclusion structure, and the interior of the inclusion stains positively for μ2 by confocal immunofluorescence microscopy, we think that this possibility is unlikely.

Results presented in this report indicate that σNS facilitates an important early step in reovirus replication that is coincident with its proper subcellular localization. It is probable that σNS interacts with other viral proteins, such as μNS and σ3, and perhaps with cellular proteins, such as cytoskeletal or translational components, to nucleate sites of viral replication. Our findings suggest that once these sites have been established, proteins required for RNA synthesis, such as μ2, are recruited to commence dsRNA synthesis. At this time in viral replication, other structural proteins would also localize to these sites to complete virion assembly, resulting in an inclusion replete with progeny virions. Our ongoing work will focus on mechanisms by which σNS initiates sites of viral assembly and reorganizes the intracellular environment to facilitate reovirus replication.

ACKNOWLEDGMENTS

We express our appreciation to Mark Denison, Anne Gibson Bost, and Jonathan Sheehan for essential discussions and to Jim Chappell, Mark Denison, Todd Graham, Michelle Mochow-Grundy, Jim Patton, Tim Peters, and Earl Ruley for reviews of the manuscript. We thank Laresha Bland for excellent administrative assistance and Ken Tyler for providing μ1/μ1C-specific MAb 8H6.

This work was supported by Public Health Service awards T32 GM08554 (M.M.B.) and T32 GM07347 (G.S.B. and S.E.R.) from the National Institute of General Medical Sciences, Public Health Service award AI32539 from the National Institute of Allergy and Infectious Diseases, the Turner Scholars Program (T.S.D.), and the Elizabeth B. Lamb Center for Pediatric Research. Additional support was provided by grant MT-11630 from the Medical Research Council of Canada (K.M.C.), grant 0GP0041771 from the Natural Sciences and Engineering Research Council of Canada (E.G.B.), and Public Health Service awards DK20593 to the Vanderbilt Diabetes Research and Training Center and CA68485 and DK20593 to the Vanderbilt Cell Imaging Resource.

REFERENCES

1. **Ahmed, R., P. R. Chakraborty, and B. N. Fields.** 1980. Genetic variation during lytic reovirus infection: high-passage stocks of wild-type reovirus contain temperature-sensitive mutants. J. Virol. **34:**285–287.
2. **Ahmed, R., R. S. Kauffman, and B. N. Fields.** 1983. Genetic variation during persistent reovirus infection: isolation of cold-sensitive and temperature-sensitive mutants from persistently infected L cells. Virology **131:**71–78.
3. **Antczak, J. B., and W. K. Joklik.** 1992. Reovirus genome segment assortment into progeny genomes studied by the use of monoclonal antibodies directed against reovirus proteins. Virology **187:**760–776.
4. **Coombs, K. M.** 1996. Identification and characterization of a double-stranded RNA^{-} reovirus temperature-sensitive mutant defective in minor core protein μ2. J. Virol. **70:**4237–4245.
5. **Coombs, K. M.** 1998. Stoichiometry of reovirus structural proteins in virus, ISVP, and core particles. Virology **243:**218–228.
6. **Coombs, K. M.** 1998. Temperature-sensitive mutants of reovirus. Curr. Top. Microbiol. Immunol. **233:**69–107.
7. **Coombs, K. M., S.-C. Mak, and L. D. Petrycky-Cox.** 1994. Studies of the major reovirus core protein μ2: reversion of the assembly-defective mutant *ts*C447 is an intragenic process and involves back mutation of Asp-383 to Asn. J. Virol. **68:**177–186.
8. **Cross, R. K., and B. N. Fields.** 1972. Temperature-sensitive mutants of reovirus type 3: studies on the synthesis of viral RNA. Virology **50:**799–809.
9. **Fields, B. N., and W. K. Joklik.** 1969. Isolation and preliminary genetic and biochemical characterization of temperature-sensitive mutants of reovirus. Virology **37:**335–342.
10. **Fields, B. N., R. Laskov, and M. D. Scharff.** 1972. Temperature-sensitive mutants of reovirus type 3: studies on the synthesis of peptides. Virology **50:**209–215.
11. **Fields, B. N., C. S. Raine, and S. G. Baum.** 1971. Temperature-sensitive mutants of reovirus type 3: defects in viral maturation as studied by immunofluorescence and electron microscopy. Virology **43:**569–578.
12. **Gillian, A. L., and M. L. Nibert.** 1998. Amino terminus of reovirus nonstructural protein σNS is important for ssRNA binding and nucleoprotein complex formation. Virology **240:**1–11.
13. **Gomatos, P. J., O. Prakash, and N. M. Stamatos.** 1981. Small reovirus particles composed solely of sigma NS with specificity for binding different nucleic acids. J. Virol. **39:**115–124.
14. **Gomatos, P. J., I. Tamm, S. Dales, and R. M. Franklin.** 1962. Reovirus type 3: physical characteristics and interactions with L cells. Virology **17:**441–454.
15. **Goral, M. I., M. Mochow-Grundy, and T. S. Dermody.** 1996. Sequence diversity within the reovirus S3 gene: reoviruses evolve independently of host species, geographic locale, and date of isolation. Virology **216:**265–271.
16. **Hazelton, P. R., and K. M. Coombs.** 1995. The reovirus mutant tsA279 has temperature-sensitive lesions in the M2 and L2 genes: the M2 gene is associated with decreased viral protein production and blockade in transmembrane transport. Virology **207:**46–58.

17. **Huismans, H., and W. K. Joklik.** 1976. Reovirus-coded polypeptides in infected cells: isolation of two native monomeric polypeptides with high affinity for single-stranded and double-stranded RNA, respectively. Virology **70:**411–424.
18. **Joklik, W. K., and M. R. Roner.** 1995. What reassorts when reovirus genome segments reassort? J. Biol. Chem. **270:**4181–4184.
19. **Mbisa, J. L., M. M. Becker, S. Zou, T. S. Dermody, and E. G. Brown.** 2000. Reovirus μ2 protein determines strain-specific differences in the rate of viral inclusion formation in L929 cells. Virology **272:**16–26.
20. **McCrae, M. A., and W. K. Joklik.** 1978. The nature of the polypeptide encoded by each of the ten double-stranded RNA segments of reovirus type 3. Virology **89:**578–593.
21. **Morgan, E. M., and H. J. Zweerink.** 1977. Characterization of the double-stranded RNA in replicase particles in reovirus infected cells. Virology **77:**421–423.
22. **Morgan, E. M., and H. J. Zweerink.** 1975. Characterization of transcriptase and replicase particles isolated from reovirus infected cells. Virology **68:**455–466.
23. **Mustoe, T. A., R. F. Ramig, A. H. Sharpe, and B. N. Fields.** 1978. A genetic map of reovirus. III. Assignment of the double-stranded RNA mutant groups A, B, and G to genome segments. Virology **85:**545–556.
24. **Mustoe, T. A., R. F. Ramig, A. H. Sharpe, and B. N. Fields.** 1978. Genetics of reovirus: identification of the dsRNA segments encoding the polypeptides of the μ and σ size classes. Virology **89:**594–604.
25. **Nibert, M. L., L. A. Schiff, and B. N. Fields.** 1996. Reoviruses and their replication, p. 1557–1596. *In* B. N. Fields, D. M. Knipe, and P. M. Howley (ed.), Fields virology, 3rd ed. Lippincott-Raven, Philadelphia, Pa.
26. **Noble, S., and M. L. Nibert.** 1997. Core protein μ2 is a second determinant of nucleoside triphosphatase activities by reovirus cores. J. Virol. **71:**7728–7735.
27. **Piron, M., P. Vende, J. Cohen, and D. Poncet.** 1998. Rotavirus RNA-binding protein NSP3 interacts with eIF4GI and evicts the poly(A) binding protein from eIF4F. EMBO J. **17:**5811–5821.
28. **Ramig, R., and B. N. Fields.** 1983. Genetics of reovirus, p. 197–228. *In* W. Joklik (ed.), The Reoviridae. Plenum Press, New York, N.Y.
29. **Ramig, R. F., R. Ahmed, and B. N. Fields.** 1983. A genetic map of reovirus: assignment of the newly defined mutant groups H, I, and J to genome segments. Virology **125:**299–313.
30. **Ramig, R. F., T. A. Mustoe, A. H. Sharpe, and B. N. Fields.** 1978. A genetic map of reovirus. II. Assignment of the double-stranded RNA-negative mutant groups C, D, and E to genome segments. Virology **85:**531–534.
31. **Rhim, J. S., L. E. Jordan, and H. D. Mayor.** 1962. Cytochemical, fluorescent-antibody and electron microscopic studies on the growth of reovirus (ECHO 10) in tissue culture. Virology **17:**342–355.
32. **Richardson, M. A., and Y. Furuichi.** 1985. Synthesis in *Escherichia coli* of the reovirus nonstructural protein σ_{NS}. J. Virol. **56:**527–533.
33. **Rodgers, S. E., J. L. Connolly, J. D. Chappell, and T. S. Dermody.** 1998. Reovirus growth in cell culture does not require the full complement of viral proteins: identification of a σ1s-null mutant. J. Virol. **72:**8597–8604.
34. **Schmechel, S., M. Chute, P. Skinner, R. Anderson, and L. Schiff.** 1997. Preferential translation of reovirus mRNA by a σ3-dependent mechanism. Virology **232:**62–73.
35. **Sharpe, A. H., L. B. Chen, and B. N. Fields.** 1982. The interaction of mammalian reoviruses with the cytoskeleton of monkey kidney CV-1 cells. Virology **120:**399–411.
36. **Silverstein, S. C., and P. H. Schur.** 1970. Immunofluorescent localization of double-stranded RNA in reovirus-infected cells. Virology **41:**564–566.
37. **Skup, D., and S. Millward.** 1980. mRNA capping enzymes are masked in reovirus progeny subviral particles. J. Virol. **34:**490–496.
38. **Skup, D., H. Zarbl, and S. Millward.** 1981. Regulation of translation in L-cells infected with reovirus. J. Mol. Biol. **151:**35–55.
39. **Stamatos, N. M., and P. J. Gomatos.** 1982. Binding to selected regions of reovirus mRNAs by a nonstructural reovirus protein. Proc. Natl. Acad. Sci. USA **79:**3457–3461.
40. **Stempek, J. G., and R. T. Ward.** 1964. An improved staining method for electron microscopy. J. Cell Biol. **22:**697–701.
41. **Venable, J. H., and R. Coggeshall.** 1965. A simplified lead citrate stain for use in electron microscopy. J. Cell Biol. **25:**407–408.
42. **Virgin, H. W., IV, M. A. Mann, B. N. Fields, and K. L. Tyler.** 1991. Monoclonal antibodies to reovirus reveal structure/function relationships between capsid proteins and genetics of susceptibility to antibody action. J. Virol. **65:**6772–6781.
43. **Watanabe, Y., S. Millward, and A. F. Graham.** 1968. Regulation of transcription of the reovirus genome. J. Mol. Biol. **36:**107–123.
44. **Watanabe, Y., L. Prevec, and A. F. Graham.** 1967. Specificity in transcription of the reovirus genome. Proc. Natl. Acad. Sci. USA **58:**1040–1047.
45. **Wiener, J. R., and W. K. Joklik.** 1987. Comparison of the reovirus serotype 1, 2, and 3 S3 genome segments encoding the nonstructural protein σNS. Virology **161:**332–339.
46. **Yin, P., M. Cheang, and K. M. Coombs.** 1996. The M1 gene is associated with differences in the temperature optimum of the transcriptase activity in reovirus core particles. J. Virol. **70:**1223–1227.
47. **Zarbl, H., and S. Millward.** 1983. The reovirus multiplication cycle, p. 107–196. *In* W. K. Joklik (ed.), The Reoviridae. Plenum Press, New York, N.Y.
48. **Zarbl, H., D. Skup, and S. Millward.** 1980. Reovirus progeny subviral particles synthesize uncapped mRNA. J. Virol. **34:**497–505.
49. **Zou, S., and E. G. Brown.** 1996. Stable expression of the reovirus μ2 protein in mouse L cells complements the growth of a reovirus ts mutant with a defect in its M1 gene. Virology **217:**42–48.
50. **Zweerink, H. J., E. M. Morgan, and J. S. Skyler.** 1976. Reovirus morphogenesis: characterization of subviral particles in infected cells. Virology **73:**442–453.